ACS OMEGA

http://pubs.acs.org/journal/acsodf

Article

Laser-Induced Shockwave Crystallization in Supersaturated Solutions and Conceivable Clustering in Undersaturated Aqueous Potassium Nitrate Solutions

Yusron Darojat, Abdulaziz Aljalal, Khaled Gasmi, Isam H. Aljundi, Nasrin Mirsaleh-Kohan, and Watheq Al-Basheer*

Cite This: *ACS Omega* 2022, 7, 38400−38408

Read Online

ACCESS | Metrics & More | Article Recommendations | Supporting Information

ABSTRACT: In this study, a newly developed setup based on laser-induced shockwave crystallization coupled with electric conductivity monitoring was employed to study the growth of crystals in supersaturated solutions and to investigate possible clustering in undersaturated solutions of potassium nitrate (KNO_3). A comparison was drawn between crystals induced by laser irradiation, by shockwaves, and spontaneously in terms of crystals' mean size, shape, and size distribution. The size distribution of produced crystals by shockwaves was also characterized in terms of laser irradiation time. The results show that produced crystals by shockwaves propagation have the sharpest size distribution and the smallest mean dimensions compared to crystals grown spontaneously or by direct laser induction. Real-time monitoring of nucleation was also performed in supersaturated solutions, while decrease in conductivity was observed in undersaturated solutions as a function of laser irradiation time.

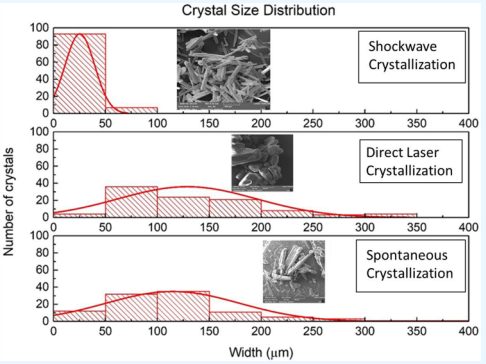

I. INTRODUCTION

Nowadays, crystallization is one of the most utilized physicochemical processes in many industries dedicated to the fabrication of high-end solid products. In principle, spontaneous crystallization can occur in supersaturated solutions.[1,2] However, crystals grown spontaneously could require extended time to grow and are known to have a wide distribution of shape and size, which limits their usage and applications. For crystallization to occur nonspontaneously in supersaturated solutions, a stimulating perturbation is required to trigger nucleation of crystals in an ordered fashion.[3] In literature, various experimental techniques have been employed to initiate perturbation in solutions and to nucleate crystals, such as beta particles irradiation,[4] sonication,[5] and light irradiation.[6−24] Laser-induced crystallization is a well-known light irradiation method in which intense laser pulses or tightly focused continuous-wave (CW) beams are applied in a solution to trigger nucleation. Laser-induced crystallization can be either direct if laser pulses are directed into the solution or, otherwise, indirect if laser pulses have no contact with the solution. The laser wavelength and polarization play a significant role in the former experimental setting,[6,23,25−27] whereas generated shock waves, bubble formations, and cavitation bubbles drive crystallization in the latter setting.[22] In a landmark publication,[6] Garetz and co-workers reported a new photophysical phenomenon in which 1064 nm laser pulses were employed to induce crystallization in an aqueous supersaturated urea solution. Later on, Garetz and co-workers concluded that non-photochemical laser-induced nucleation (NPLIN) in lysozyme solutions was more effective when using intense 532 nm laser pulses of short duration over a shorter aging time.[8] Subsequently, direct laser-induced crystallization and growth in benzophenone[10] and anthracene[11] solutions were investigated by Okutsu et al. by utilizing ultraviolet laser pulses. Strikingly, the first example of a photochemical morphology control of a crystal was reported by the same group.[10] Hosokawa and co-workers used a single femtosecond laser pulse to induce crystallization in different organic supersaturated solutions[16−18] and determined that the crystallization efficiency was higher than that using a nanosecond laser.[17] Furthermore, they suggested that the crystallization mechanism was completely different[16] from that reported previously based on photochemical reactions or molecular alignment due to a strong optical field. Hosokawa and co-workers further concluded that the nucleation depended on the laser repetition rate.[17] More studies followed on laser-induced crystallization of L-histidine,[19] potassium chloride,[20] and KCl in agarose gel.[21] In a recent study, Yuyama

Received: June 2, 2022
Accepted: October 13, 2022
Published: October 24, 2022

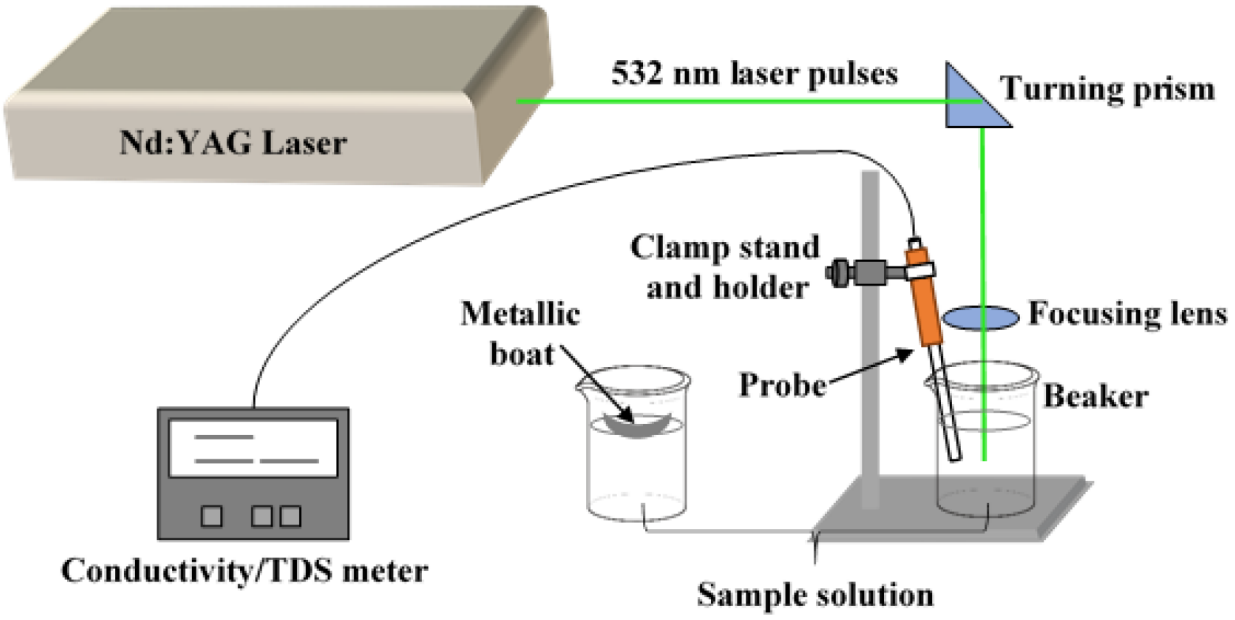

Figure 1. A sketch of the main components of the experimental setup used to induce crystallization in aqueous KNO_3 solutions.

et al.[24] employed tightly focused CW laser beams in the near-infrared region with laser trapping in unsaturated aqueous solution. In that study, two-dimensional growth rate control of single L-phenylalanine plate-like anhydrous crystal was demonstrated.[24]

Recently, Mirsaleh-Kohan et al. reported indirect laser-induced shockwave crystallization of sodium chloride, tartaric acid, and sodium bromate in supersaturated aqueous solutions using a new technique.[22] In their new technique, sound and shockwaves were generated by impinging 532 nm laser pulses on a metallic surface. As a result, the propagating shockwaves can produce many tiny crystals of length dimension much less than 1 mm. They concluded that generated sound and shockwaves yielded small crystals at an early stage of growth, which can be regarded as seeds for the growth of bigger crystals.

In this work, we further explore the growth of small crystals in aqueous potassium nitrate by making a modification to the setup reported in ref 22 so as to allow the real-time monitoring of electrical conductivity. Potassium nitrate was selected due to its high solubility in water, abundance, and application in many industries, such as food,[28] agriculture,[29] dyes,[30] and solar cell doping.[31] We present a comparison of size, shape, and size distribution of crystals grown spontaneously, by direct laser irradiation, and by pure shockwaves.

Clusters that might form in undersaturated solutions are unstable and too small for extraction from the large solution volume. An alternative and experimentally challenging approach is to monitor cluster growth in real-time while still in solution. We report the real-time monitoring of laser-induced crystallization in supersaturated solutions and possible clustering in undersaturated KNO_3 solutions using electrical conductivity as a probe, based on the fact that clustering and crystal growth will reduce the concentration of free ions in the solution.

II. EXPERIMENTAL METHODS

Figure 1 shows a sketch of the experimental setup used to induce crystallization in aqueous solutions of potassium nitrate by nanosecond laser pulses.

The laser used was a Nd:YAG laser (Quanta Ray-*PRO* series from Spectra-Physics) generating pulses of 532 nm, 5 ns, and 10 Hz, laser wavelength, pulse duration, and repetition rate, respectively. Laser pulses were vertically directed downward using a turning prism and then focused into the center of the solution container using a 50 mm plano-convex lens. The observed optimal laser energy for crystallization was about 80 mJ/pulse. Samples of 500 mL volume of supersaturated and undersaturated aqueous solutions of potassium nitrate (KNO_3) were prepared with the aid of a magnetic stirrer. When preparing supersaturated solutions, and in addition to stirring, the solutions were heated up to 50 °C to optimize solute dissolvability. The prepared solutions were then left to cool down to room temperature. All samples were contained in a 12 cm height and 8 cm diameter beaker. Identical control samples were also prepared and left to crystallize spontaneously over the same time period as the laser irradiation time. A probe of electric conductivity meter was submerged in the solutions during laser irradiation to monitor solution conductivity in real-time. In order to detect the slightest changes to electric conductivity in the solution, the active region of the probe was suspended at about 3 mm from the laser focus within the solution body. The probe was connected to a digital EC meter (HI763100 from Hanna Instruments). The solution samples were independently exposed to laser pulses over different time periods extending from 1 to 12 min. Crystallization was achieved by two different interchangeable experimental layouts, leading to two different crystallization mechanisms. The first mechanism was based on direct laser irradiation of the solution via laser focusing into the solution. For this experimental layout, the solution temperature was about 23.20 ± 0.05 °C, and the output laser beam diameter was about 5 mm, while the peak power density at the laser focus, of focal spot size of 2×10^{-4} cm^2, was evaluated to be about 80 GW/cm^2. The laser's spot size was determined using two different

https://doi.org/10.1021/acsomega.2c03456
ACS Omega 2022, 7, 38400−38408

methods, the first method using a laser alignment paper, while the spot size was determined in the second method using a charge-coupled device (CCD) camera along with a neutral density (ND) filter. In this experimental layout, the radiation pressure at the focal spot size was calculated to be 2.7 MPa. In the second experimental layout, the crystallization mechanism was laser-induced shockwaves, which were generated by directing laser pulses to hit a thin metallic boat floating on the solution surface. Here, the laser beam diameter at the foil's surface was about 1 mm, yielding a power density of about 2 GW/cm^2. In this layout, and to avoid any breakdown at the boat surface as well as to minimize thermal effects, laser pulses were not focused on the boat surface. Instead, pulses were focused at the center of the solution container, which was a few centimeters below the boat surface. With this experimental layout, we did not observe any physical damage nor any noticeable change in the foil's or the sample's temperature of 21.10 ± 0.05 °C. When laser pulses hit the metallic boat (made of aluminum foil) transient shockwaves were generated. Because of generated shockwave propagation, highly concentrated local areas within the solution were created, which in turn can trigger nucleation and crystal growth. For each experimental layout used, three random ensembles were carefully harvested; each ensemble contains 100 produced crystals. The crystals were then characterized by a scanning electron microscope (SEM) according to their size, shape, and size distribution. When characterizing crystals' size, the length was defined as the longest dimension measured. The average size and distribution were then used in all figures. The employed SEM system was a Field Emission Scanning Electron Microscope (FE-SEM) with magnification up to 10^6×, Tescan model Lyra-3 at King Fahd University of Petroleum & Minerals.

III. RESULTS AND DISCUSSION

In principle, nucleation is triggered in solutions when the difference in the solute's chemical potential, $\Delta\mu$, between the solution (μ) and the equilibrium solid (μ_e) phases reaches a certain threshold.[32−34] This difference in the chemical potential is given as follows

$$\Delta\mu = \mu - \mu_e = RT \ln \frac{\alpha C}{\alpha_e C_e} \quad (1)$$

where R is the gas constant, T is the solution's temperature, and C and C_e are the concentrations of the solution and the equilibrium solubility, respectively, which are related by the ratio of concentrations $S = C/C_e$, customarily referred to as the saturation parameter. Solutions are said to be supersaturated when the saturation parameter, S, is greater than unity. Under the first approximation,[32] the activity coefficients of the solute in standard solution α and in saturated solution α_e can be assumed equal. The classical nucleation rate, J, is denoted in terms of the chemical potential difference given in equation 1 above. In addition, J is dependent on interfacial tension γ between the solid and solution phases, molar volume V_m of the solid phase, and temperature T via the following equation.

$$J = A \exp\left[-\left(\frac{16\pi}{3}\right)\left(\frac{\gamma^3 V_m^2}{\Delta\mu^2 k_B T}\right)\right] \quad (2)$$

Here A is a pre-exponential constant, and k_B is the well-known Boltzmann constant. As exhibited in equation 2, the nucleation rate is directly sensitive to variations in chemical potential difference $\Delta\mu$, temperature T, and γ or indirectly to any external factors that might influence these three parameters. Photochemical and non-photochemical interactions of laser light with solute particles in solution are known to locally increase pressure and temperature in the vicinity of the interaction point,[15,35] even when using a single laser pulse.[36] This in turn can lead to an increase in nucleation rate, making

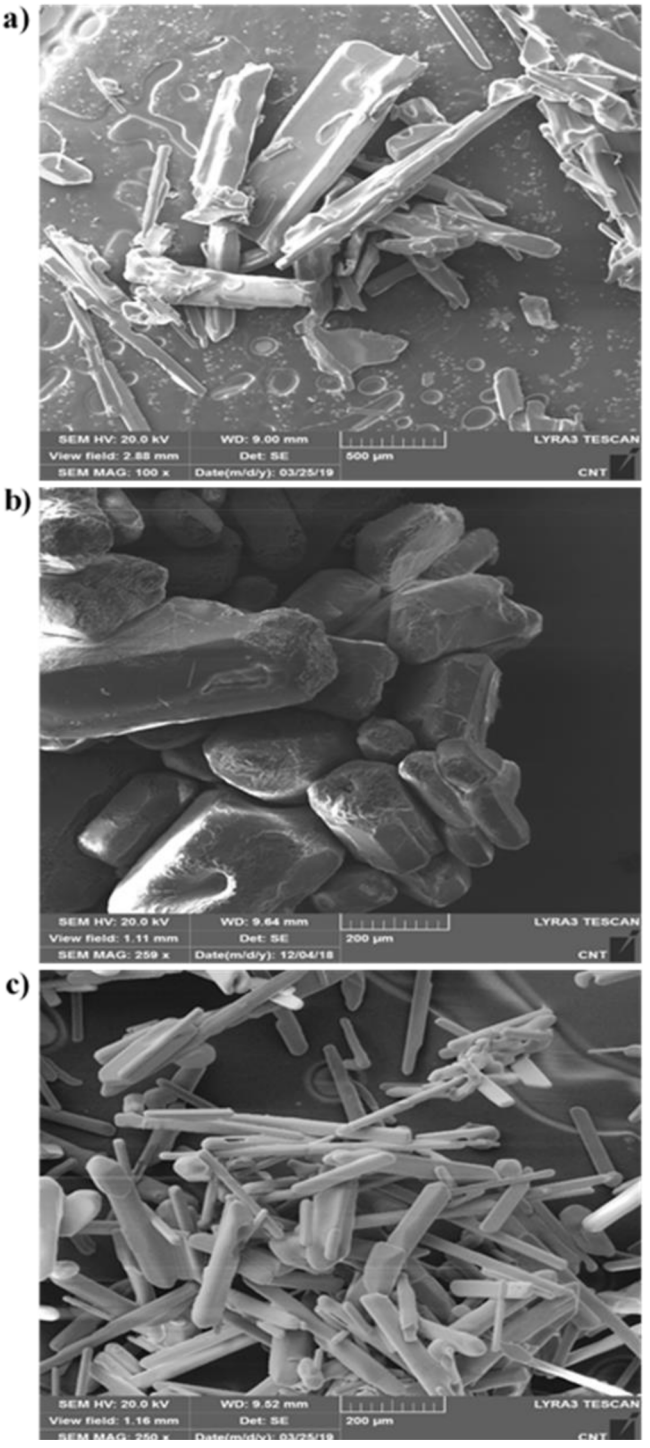

Figure 2. SEM images of the KNO_3 crystals grown after 12 min by (a) spontaneous crystallization with a scale bar of 500 μm, (b) direct laser-induced crystallization, and (c) laser-induced shockwave crystallization. The scale bar in images (b, c) is 200 μm.

https://doi.org/10.1021/acsomega.2c03456
ACS Omega 2022, 7, 38400−38408

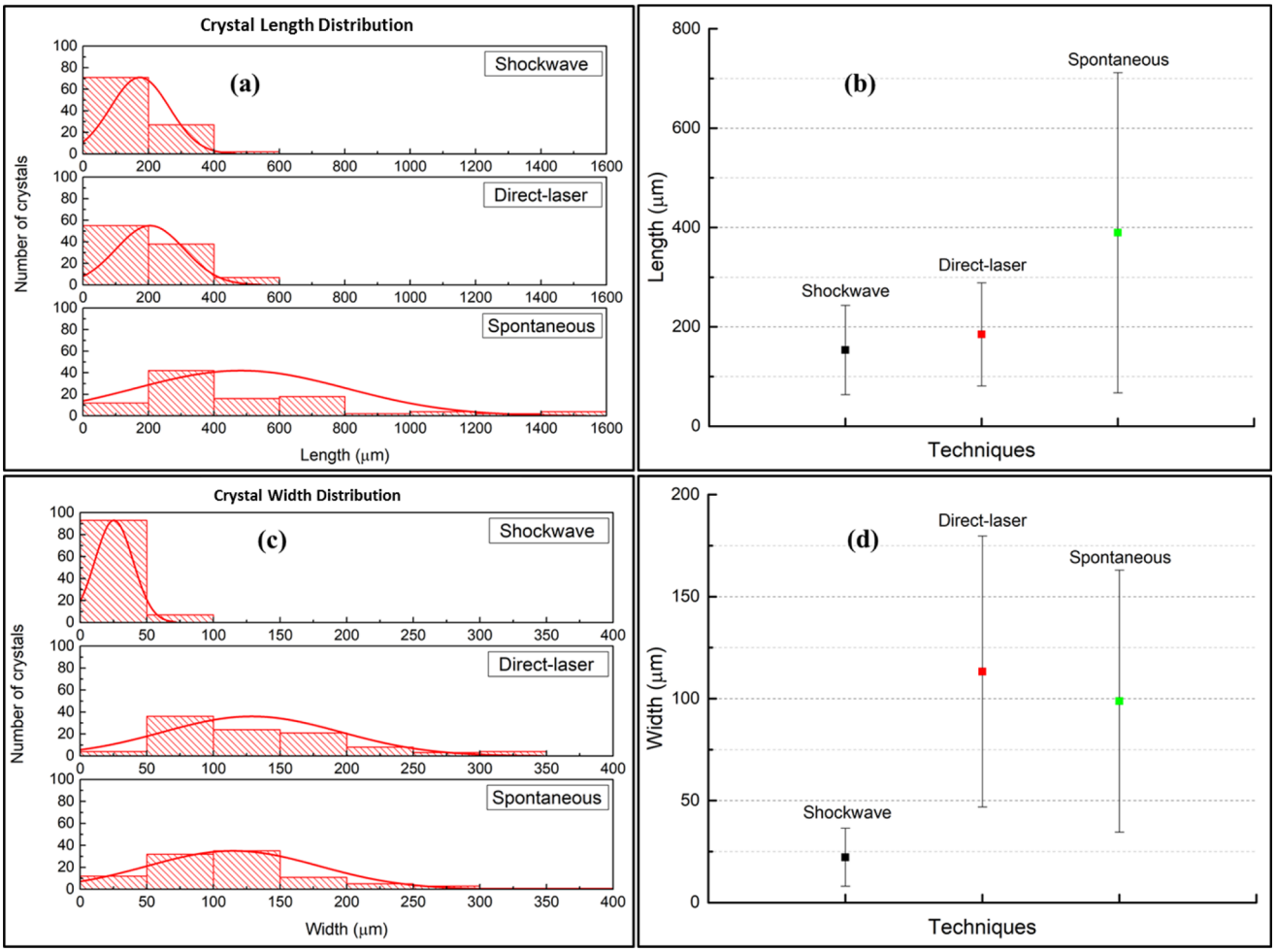

Figure 3. (a) Length distributions along with (b) the mean length and the (c) width distributions along with (d) the mean width of KNO_3 crystals grown by different techniques. The standard deviations of the mean length and width values for grown crystals' actual distributions are shown as the error bars in (b, d).

crystal growth in an ordered fashion more probable. In what follows, we will present a comparison between crystals produced spontaneously, by direct laser irradiation, and by laser-induced shockwaves.

Figure 2 shows the SEM images of the KNO_3 crystals grown spontaneously, by direct laser-induced crystallization, and by laser-induced shockwave crystallization. All crystals shown in Figure 2 were produced over the same period of time, that is, 12 min of allowing the solution to crystallize spontaneously or of irradiating the solution with the laser. The saturation level of all KNO_3 solutions used was about $S = 1.32 \pm 0.05$. This saturation level was selected as it was experimentally determined to be the threshold for spontaneous crystallization at room temperature. The crystals formed spontaneously in Figure 2a were bulky and irregular in shape with a wide size distribution of about 40−1600 μm in length and 30−300 μm in width. Figure 2b shows the SEM image of yielded crystals by direct laser focusing into the solution. Here, characterization of harvested crystals reveals a narrower size distribution than the size distribution of spontaneously grown crystals, with a range of 90−600 μm in length and 50−350 μm in width. The SEM image of Figure 2c shows a sample of crystals grown via shockwaves (metallic boat layout). Compared to crystals grown spontaneously and by direct laser irradiation, the size distribution of shockwave-grown crystals was the sharpest, extending from 60 to 400 μm in length and from 10 to 100 μm in width. It should be noted that using X-ray diffraction (XRD) analysis, all yielded crystals in this study were of the orthorhombic polymorphous structure. As crystals grown using the three aforementioned techniques can vary in size and shape, a statistical treatment of yielded crystals can be very useful in comprehending the tendency of grown crystals' size, shape, and distribution.

Figure 3 shows the grown crystal length and width distributions using the three techniques, along with mean length and width values of produced crystals for each technique.

The Gaussian fitting of the histograms of Figures 3a,c shows that the size distribution of crystals grown by pure shockwaves was the sharpest. Moreover, the displayed data suggest that, compared to direct laser-induced crystallization, shockwave crystallization tends to produce a smaller and sharper size distribution of crystals. One plausible explanation stems from the different scope of effect of these crystallization mechanisms, as pure shockwaves used in the second experimental layout were expected to affect bigger solution volume than the volume influenced by direct laser-induced crystallization. Hence, shockwave crystallization can produce many more nucleation sites than laser-induced crystallization. With time, the nucleation sites produced by shockwaves compete over the

https://doi.org/10.1021/acsomega.2c03456
ACS Omega 2022, 7, 38400−38408

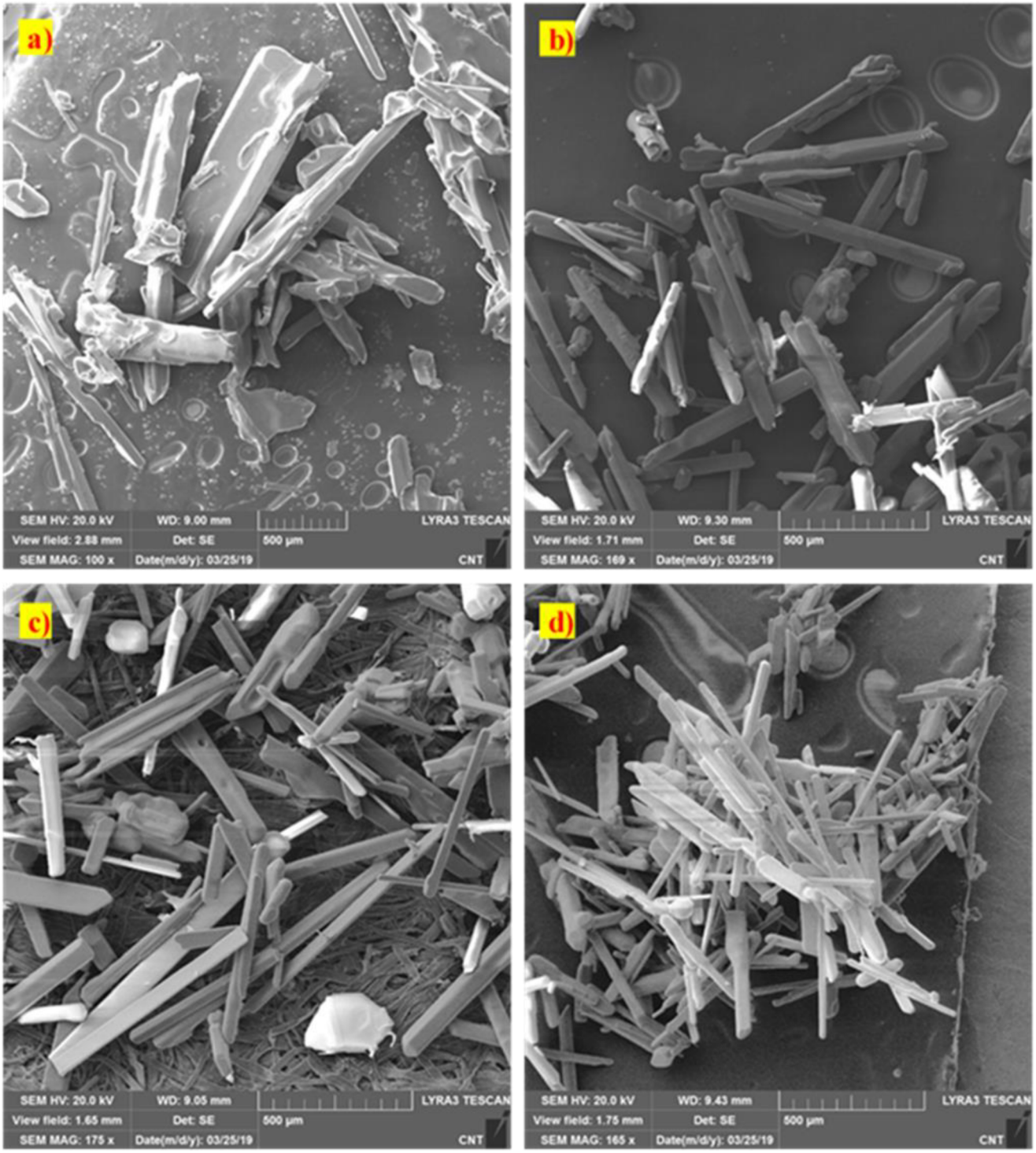

Figure 4. Wide-view SEM images of the KNO_3 crystals grown (a) spontaneously without laser after 10 min, by shockwave exposure for (b) 1, (c) 5, and (d) 10 min. The scale bar of all images was 500 μm.

excess solute in the solution. This will cause the production of many smaller crystals compared to crystals produced by direct laser induction. The data presented in Figure 3b,d demonstrate that, compared to crystals grown spontaneously and by direct laser irradiation, the mean length and width of crystals formed using pure shockwaves were observed to be the smallest with ~160 and 25 μm, respectively. It should be noted that the difference in mean length between crystals grown by direct laser irradiation and shockwave techniques, see Figure 3b, was much smaller than the difference in the mean width, see Figure 3d. One feasible explanation of this variation might be due to the breaking of a portion of yielded crystals along their brittle length in the course of harvesting and storing yielded crystals. As the process of crystal growth is time-dependent, further investigation is needed to study crystal growth dynamics as a function of laser irradiation time. When the laser irradiation time was changed during direct laser irradiation, no significant difference in the size distribution of grown crystals was

https://doi.org/10.1021/acsomega.2c03456
ACS Omega 2022, 7, 38400−38408

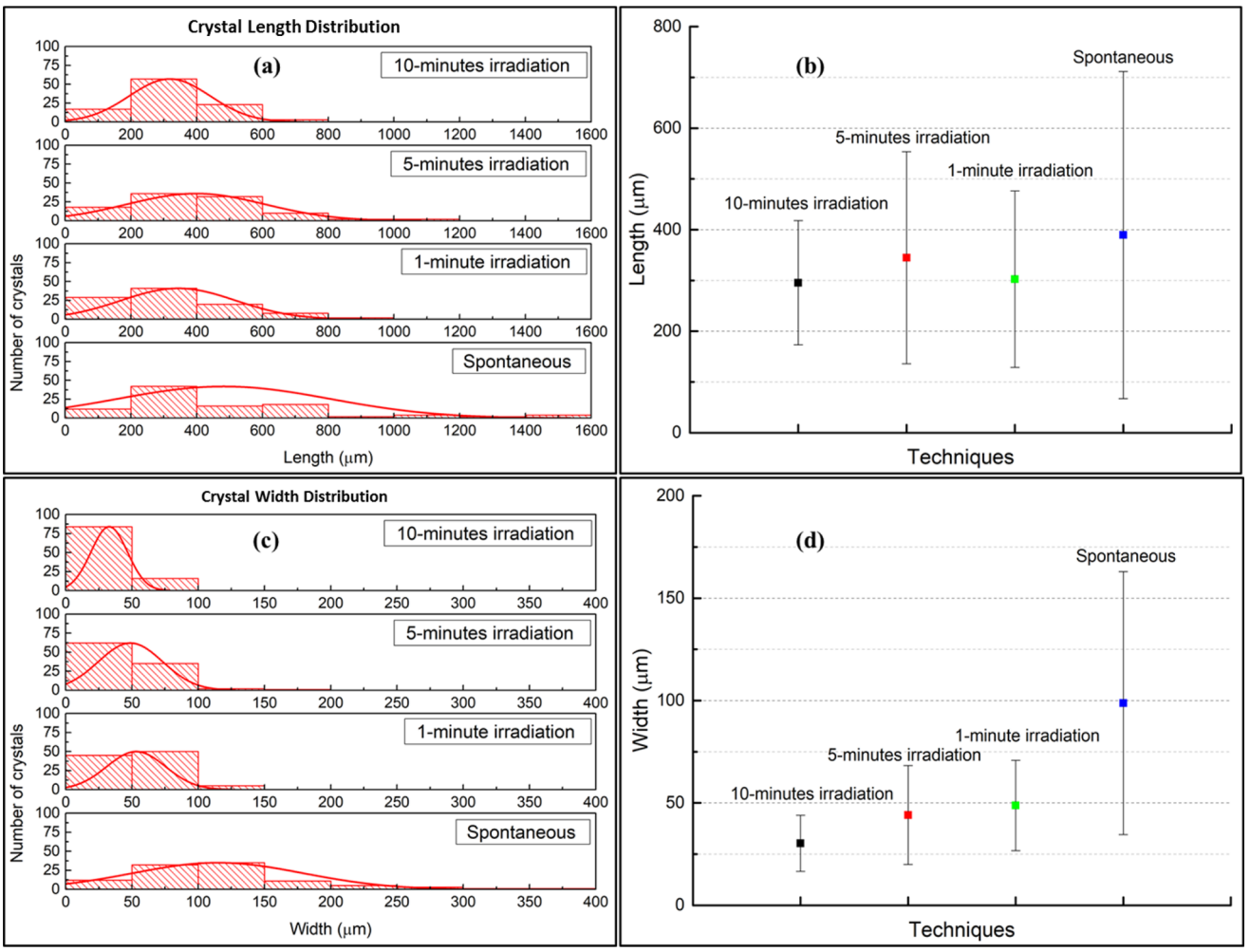

Figure 5. (a) Length distributions along with (b) the mean length and the (c) width distributions along with (d) the mean width of KNO_3 crystals grown with shockwaves at different irradiation times ranging from 1 to 10 min. The standard deviations of the mean length and width values for grown crystals' actual distributions are shown as the error bars (b, d).

observed. In the literature, Hua et al.[37] reported that changing the irradiation time during direct laser irradiation has little effect on produced crystals' size. So, our time-dependent research was focused on shockwave crystallization. Figure 4 shows the SEM image of KNO_3 crystals produced via shockwaves under the same experimental conditions of laser energy and sample concentration as Figures 2 and 3 but with varying laser irradiation times. Specifically, Figure 4a shows the wide view of SEM image of crystals yielded spontaneously, taken after 10 min of solution preparation. Figure 4b−d shows the wide-view SEM images of crystals grown using shockwaves after exposing the metallic boat to 80 mJ/pulse laser for 1, 5, and 10 min, respectively. Crystals produced after 1 min of exposure time, shown in the SEM image of Figure 4b, were regular in shape and of a size distribution ranging from 110 to 800 μm in length and 20−150 μm in width. Correspondingly, crystals produced after 5 min of laser irradiation time were also regular but of a sharper size distribution that ranges from 120 to 800 μm in length and 20−100 μm in width. On the other hand, Figure 4d shows an SEM image of crystals yielded after 10 min of laser irradiation time with the sharpest size distribution spanning over 100−600 μm in length and 20−100 μm in width.

Figure 5 exhibits the length and width size distributions of yielded KNO_3 crystals produced spontaneously and by laser-induced shockwaves at different irradiation times, along with the crystals' mean length and width values at each irradiation time.

The histograms of the number of crystals as a function of grown crystals' length and width were best fitted using a Gaussian distribution, see Figure 5a,c. The mean length and width for crystals grown spontaneously as well as by laser-induced shockwaves of different irradiation times are shown in Figure 5b,d, respectively. The grown crystals' lowest mean length and width were found to be 300 and 30 μm, respectively, for a laser induction time of 10 min. Figure 5a,c shows a general trend of sharper size distribution as a function of exposure time to laser-induced shockwave. As for the produced crystals' mean leangth and width, Figure 5b shows a slight variation in produced crystals' mean length with shockwave exposure time compared to about a 40% decrease in crystals' mean width, see Figure 5d. Additionally, there are two competing factors that could play a role in the production of smaller crystals by shockwaves. These factors are the natural crystal growth in supersaturated solutions and crystal breakage.[38,39] As the rate of breakage is slightly higher than the rate of natural growth, these two opposing effects result in the

https://doi.org/10.1021/acsomega.2c03456
ACS Omega 2022, 7, 38400−38408

production of smaller crystals with time. The competition of the aforementioned factors can cause shockwave-produced crystals to nonlinearly evolve in time. For example, when comparing the dimensions of crystals produced after 12 min, see Figure 3, with dimensions of crystals after 10 min, Figure 5, the length of shockwave-grown crystals experienced a 50% decrease over a period of 2 min. The produced crystals' elongated shape can cause the length dimension to be more vulnerable to breakage than the width dimension. It should be noted here that the yielded KNO_3 crystal dimensions using shockwaves are of the same order of magnitude as the dimensions of crystals reported by a similar experimental layout.[22]

Like all water-soluble ionic compounds, the KNO_3 molecule dissociates in water into potassium cations, K^+, and nitrate anions, NO_3^-. When nucleation is triggered in the solution, the dissolved charged free ions might couple into ion pairs, locally near to the nucleus. The ion pairs could later conglomerate to form relatively neutral clusters, causing a decrease in the overall electric conductivity of the solution. Henceforth, by employing an electric conductivity probe in the setup, real-time monitoring of clustering and the subsequent early crystallization stage is feasible. Another advantage of utilizing electric conductivity in monitoring nucleation in supersaturated solutions and clustering in undersaturated solutions is that it can offer a way of detecting the possible formation of short-lived solute clusters that might form in undersaturated aqueous solutions. Figure 6 shows the decrease in the electric

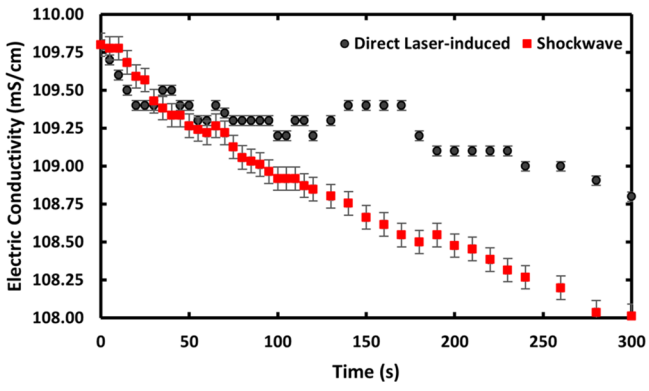

Figure 6. Measured average electric conductivity as a function of laser irradiation time in supersaturated KNO_3 solution. The black symbols represent conductivity change in the direct laser induction experimental layout. The red symbols show conductivity change in the shockwave induction of nucleation. The error bars represent the standard deviation from the average electric conductivity of three measurements.

conductivity (in mS/cm) as a function of laser irradiation time in supersaturated KNO_3 solution of saturation level S = 1.1, which corresponds to a concentration of 34.82 g/100 mL. The time frame of the experiment was relatively short, ∼300 s, to minimize the effect of undesired spontaneous nucleation. The black symbols in the figure show the solution's conductivity when laser pulses are directly focused into the solution, whereas the conductivity when laser pulses are directed to hit the metallic boat is exhibited as the red symbols.

Also shown in Figure 6 is a clear trend of a steeper decrease in conductivity (ca. −1.6%) when nucleation was triggered by the shockwaves, compared to only −0.6% decrease in conductivity in direct laser induction. An interesting feature in electric conductivity when direct laser induction was used is the sudden drop at 20 s, which was observed to last for some time. This drop in electric conductivity might be due to the creation of many nucleation centers in the vicinity of the probe. It should be noted that there are other possible and competing mechanisms that can influence the solution's electric conductivity. These mechanisms are difficult to exclude due to experimental limitations and involve thermal heating, degassing, bubble formations, and cavitation. Based on the promising results of Figure 6, the same measurement was also performed in undersaturated solutions. It should be mentioned that investigating clustering in undersaturated solutions might yield useful information, since spontaneous nucleation can never occur in undersaturated solutions. Figure 7 shows the

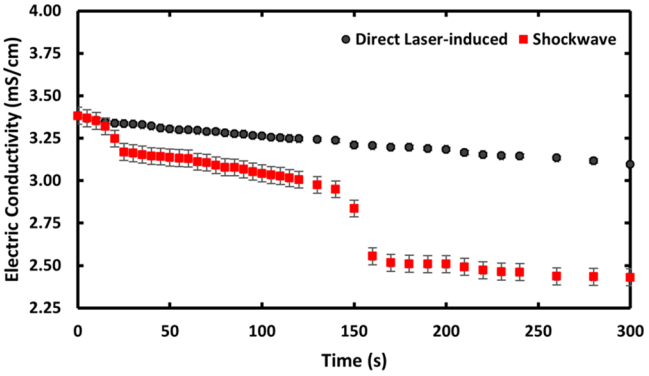

Figure 7. Measured average electric conductivity as a function of laser irradiation time in undersaturated KNO_3 solution at saturation level S = 0.03. The black symbols represent conductivity change in the direct laser induction experimental layout. The red symbols show conductivity change in the shockwave induction of clustering. The error bars represent the standard deviation from the average electric conductivity of three measurements.

electric conductivity measured in undersaturated KNO_3 solution of saturation level S = 0.03, which corresponds to a solution concentration of 0.95 g/100 mL. The measurement was performed over the same period of time as for the experiment with supersaturated solution, shown in Figure 6.

We observed a clear trend in the steeper decrease in conductivity (ca. −28%) when the solution was exposed to the shockwaves, compared to only −4.0% decrease in conductivity by direct laser induction. It is worth mentioning that direct laser hits into the solution can cause local heating, which could have the opposite and competing effect to clustering by increasing conductivity due to the disintegration of neutral clusters. This could explain the sharper decrease in conductivity in shockwave-induced nucleation compared to direct-laser-induced nucleation. In a shockwave layout, where laser pulses are not in contact with the solution body, local heating could also occur due to transport of heat from the foil's surface to the solution's body via convection. Nevertheless, we have not observed any significant change in the solution's temperature over the experiment time frame of 300 s. This was not surprising, as the role of local heating in this layout is expected to be less than that in direct laser layout due to the nature of the convection process as well as due to the relatively large solution volume. Another observed feature in the electric conductivity of the shockwave is the early drop in electric conductivity at 20 s and then a much steeper drop in conductivity at 140 s. There are few possible explanations for

https://doi.org/10.1021/acsomega.2c03456
ACS Omega 2022, 7, 38400−38408

the drops in conductivity in Figures 6 and 7. The first explanation could be as an outcome of forming many clustering centers or due to the creation of a local bubble, chemical reactions, degassing, or cavitation in the vicinity of the electric conductivity sensor. Another feasible reason for the observed conductivity decrease with time could be related to the concentration of free ions in undersaturated solutions, which is significantly smaller than concentration in supersaturated solution. At equilibrium, the undersaturated potassium nitrate solution has a mixture of free ions and ion pairs, owing to the competing forces of diffusion and electrostatic attraction. It is possible that the propagation of laser-induced shockwaves in the solution causes an increase in the concentration of ion pairs at the expense of free ions, which would reduce the conductivity. This explanation might explain the drop of electric conductivity in undersaturated solutions. Generally, it was observed that the measured conductivity values were less than tabulated values in the *CRCHandbook*. A plausible explanation for this discrepancy could originate from the fact that the probe used is measuring conductivity in the small solution volume, which is within the proximity of the probe's active region. This small volume is near the center of the laser focus, in the case of direct laser induction, and directly below the metallic boat in the case of shockwave induction. As a result, the conductivity of this localized small volume could have lower values compared to other regions of the solution. This could explain the noticeable sensitivity of the conductivity probe in undersaturated solutions, despite their small number density of ions.

CONCLUSION

In summary, a pulsed nanosecond laser at 532 nm was employed in an experimental setup to grow crystals in aqueous solutions of potassium nitrate using two experimental layouts. The first layout involves direct laser irradiation of the solution. In the second layout, pure laser-induced shockwaves were employed to initiate nucleation in supersaturated solutions and clustering in undersaturated solutions. Using SEM imaging, the produced crystals were characterized in terms of their size distribution and mean size. Crystals grown by these two experimental layouts were also compared with the bulky and irregular crystals grown spontaneously using control samples. It was found that crystals produced by shockwave propagation have the sharpest size distribution and the smallest mean dimensions compared to crystals grown by direct laser induction or spontaneously. The time-dependent data of a laser-induced shockwave show a general trend of sharper size distribution as a function of exposure time. However, small variations were observed in the produced crystals' mean size upon increasing the shockwave's exposure time. The decrease in electric conductivity as a function of time in both supersaturated and undersaturated potassium nitrate solutions was steeper using shockwave than using direct laser induction. Nevertheless, the tendency of electric conductivity to decrease with time of laser irradiation or shockwave was attributed to few possible mechanisms. Definitely, future experimental and theoretical work is much needed to conclusively understand the specific mechanisms of nucleation in supersaturated solutions and clustering in undersaturated solutions.

ASSOCIATED CONTENT

Supporting Information

The Supporting Information is available free of charge at https://pubs.acs.org/doi/10.1021/acsomega.2c03456.

Length vs number of crystals, Width vs number of crystals, Length vs number of crystals produced by laser-induced shockwave for different irradiation time, Width vs number of crystals produced by laser-induced shockwave for different irradiation time, Time vs electric conductivity for S = 1.1, Time vs electric conductivity for S = 0.03 (PDF)

AUTHOR INFORMATION

Corresponding Author

Watheq Al-Basheer − *Department of Physics, King Fahd University of Petroleum & Minerals, Dhahran 31261, Saudi Arabia; Interdisciplinary Research Center of Membranes and Water Security, King Fahd University of Petroleum & Minerals, Dhahran 31261, Saudi Arabia;* orcid.org/0000-0002-2100-9333; Phone: +966-13-860-2216; Email: Watheq@kfupm.edu.sa; Fax: +966 13 860 2293

Authors

Yusron Darojat − *Department of Physics, King Fahd University of Petroleum & Minerals, Dhahran 31261, Saudi Arabia; Department of Physics, Institut Teknologi Sumatera, Lampung 35365, Indonesia*

Abdulaziz Aljalal − *Department of Physics, King Fahd University of Petroleum & Minerals, Dhahran 31261, Saudi Arabia*

Khaled Gasmi − *Department of Physics, King Fahd University of Petroleum & Minerals, Dhahran 31261, Saudi Arabia; Interdisciplinary Research Center for Intelligent Manufacturing and Robotics, King Fahd University of Petroleum & Minerals, Dhahran 31261, Saudi Arabia*

Isam H. Aljundi − *Chemical Engineering Department, King Fahd University of Petroleum and Minerals, Dhahran 31261, Saudi Arabia; Interdisciplinary Research Center of Membranes and Water Security, King Fahd University of Petroleum & Minerals, Dhahran 31261, Saudi Arabia;* orcid.org/0000-0002-0714-8580

Nasrin Mirsaleh-Kohan − *Division of Chemistry and Biochemistry, Texas Woman's University, Denton 76204 Texas, United States;* orcid.org/0000-0001-9655-9711

Complete contact information is available at: https://pubs.acs.org/10.1021/acsomega.2c03456

Notes

The authors declare no competing financial interest.

ACKNOWLEDGMENTS

The authors acknowledge the support provided by the King Fahd University of Petroleum and Minerals for funding this research under Research Grant (#DF191010).

REFERENCES

(1) Mersmann, A.*Crystallization Technology Handbook;*Marcel Dekker: New York, 2001.

(2) Kashchiev, D.*Nucleation Basic Theory with Applications;*Butterworth-Heinemann: Oxford, UK, 2000.

(3) Khamskii, E. V.*Crystallization from solutions;*Consultants Bureau: New York, 1969.

(4) Mahurin, S.; McGinnis, M.; Bogard, J. S.; Hulett, L. D.; Pagni, R. M.; Compton, R. N. Effect of beta radiation on the crystallization of sodium chlorate from water: a new type of asymmetric synthesis. *Chirality* **2001**, *13*, 636−640.
(5) Pokroy, B.; Aichmayer, B.; Schenk, A. S.; Haimov, B.; Kang, S. H.; Fratzl, P.; Aizenberg, J. Sonication-Assisted Synthesis of Large, High-Quality Mercury Thiolate Single Crystals Directly from Liquid Mercury. *J. Am. Chem. Soc.* **2010**, *132* (41), 14355−14357.
(6) Garetz, B. A.; Aber, J. E.; Goddard, N. L.; Young, R. G.; Myerson, A. S. Nonphotochemical, Polarization-Dependent, Laser-Induced Nucleation in Supersaturated Aqueous Urea Solutions. *Phys. Rev. Lett.* **1996**, *77*, 3475−3476.
(7) Zaccaro, J.; Matic, J.; Myerson, A. S.; Garetz, B. A. Nonphotochemical, laser-induced nucleation of supersaturated aqueous glycine produced unexpected γ-polymorph. *Cryst. Growth Des.* **2001**, *1*, 5−8.
(8) Lee, I. S.; Evans, J. M. B.; Erdemir, D.; Lee, A. Y.; Garetz, B. A.; Myerson, A. S. Nonphotochemical Laser Induced Nucleation of Hen Egg White Lysozyme Crystals. *Cryst. Growth Des.* **2008**, *8* (12), 4255−4261.
(9) Oxtoby, D. W. "Crystals in a flash,". *Nature* **2002**, *420*, 277−278.
(10) Okutsu, T.; Nakamura, K.; Haneda, H.; Hiratsuka, H. Laser-Induced Crystal Growth and Morphology Control of Benzopinacol Produced from Benzophenone in Ethanol/Water Mixed Solution. *Cryst. Growth Des.* **2004**, *4* (1), 113−115.
(11) Okutsu, T.; Isomura, K.; Kakinuma, N.; Horiuchi, H.; Unno, M.; Matsumoto, H.; Hiratsuka, H. Laser-Induced Morphology Control and Epitaxy of Dipara-anthracene Produced from the Photochemical Reaction of Anthracene. *Cryst. Growth Des.* **2005**, *5* (2), 461−465.
(12) Fischer, A.; Pagni, R. M.; Compton, R. N.; Kondepudi, D.*Laser-Induced Crystallization, in Nanoclusters: A Bridge Across Disciplines;*Elsevier, 2010; pp 343−364.
(13) Vogel, A.; Busch, S.; Parlitz, U. Shock wave emission and cavitation bubble generation by picosecond and nanosecond optical breakdown in water. *J. Acoust. Soc. Am.* **1996**, *100*, 148−165.
(14) Scammon, R. J.; Chapyak, E. J.; Godwin, R. P.; Vogel, A. Simulations of shock waves and cavitation bubbles produced in water by picosecond and nanosecond laser pulses. *Proc. SPIE* **1998**, *3254*, 264−275.
(15) Soare, A.; Dijkink, R.; Pascual, M. R.; Sun, C.; Cains, P. W.; Lohse, D.; Stankiewicz, A. I.; Kramer, H. J. M. Crystal Nucleation by Laser-Induced Cavitation. *Cryst. Growth Des.* **2011**, *11*, 2311−2316.
(16) Nakamura, K.; Hosokawa, Y.; Masuhara, H. Anthracene Crystallization Induced by Single-Shot Femtosecond Laser Irradiation: Experimental Evidence for the Important Role of Bubbles. *Cryst. Growth Des.* **2007**, *7* (5), 885−889.
(17) Hosokawa, Y.; Adachi, H.; Yoshimura, M.; Mori, Y.; Sasaki, T.; Masuhara, H. Femtosecond Laser-Induced Crystallization of 4-(Dimethylamino)-N-methyl-4-stilbazolium Tosylate. *Cryst. Growth Des.* **2005**, *5* (3), 861−863.
(18) Yoshikawa, H. Y.; Hosokawa, Y.; Masuhara, H. Spatial Control of Urea Crystal Growth by Focused Femtosecond Laser Irradiation. *Cryst. Growth Des.* **2006**, *6* (1), 302−305.
(19) Sun, X.; Garetz, B. A.; Myerson, A. S. Polarization Switching of Crystal Structure in the Nonphoto-chemical Laser-Induced Nucleation of Supersaturated Aqueous L-Histidine. *Cryst. Growth and Des.* **2008**, *8* (5), 1720−1722.
(20) Ward, M. R.; Ballingall, I.; Costen, M. L.; McKendrick, K. G.; Alexander, A. J. Nanosecond pulse width dependence of non-photochemical laser-induced nucleation of potassium chloride. *Chem. Phys. Lett.* **2009**, *481*, 25−28.
(21) Duffus, C.; Camp, P. J.; Alexander, A. J. Spatial Control of Crystal Nucleation in Agarose Gel. *J. Am. Chem. Soc.* **2009**, *131* (33), 11676−11677.
(22) Mirsaleh-Kohan, N.; Fischer, A.; Graves, B.; Bolorizadeh, M.; Kondepudi, D.; Compton, R. N. Laser Shock Wave Induced Crystallization. *Cryst. Growth Des.* **2017**, *17*, 576−581.
(23) Gharib, S. A.; El Omar, A. K.; Naja, A.; Deniset-Besseau, A.; Denisov, S. A.; Pernot, P.; Mostafavi, M.; Belloni, J. Anisotropic Time-Resolved Dynamics of Crystal Growth Induced by a Single Laser Pulse Nucleation. *Cryst. Growth Des.* **2021**, *21*, 799−808.
(24) Yuyama, K.; George, J.; Thomas, K. G.; Sugiyama, T.; Masuhara, H. Two-Dimensional Growth Rate Control of L Phenylalanine Crystal by Laser Trapping in Unsaturated Aqueous Solution. *Cryst. Growth Des.* **2016**, *16*, 953−960.
(25) sun, Q.; Cui, S.; Zhang, M. Homogeneous Nucleation Mechanism of NaCl in Aqueous Solutions. *Crystals* **2020**, *10* (2), 107.
(26) Ward, M. R.; McHugh, S.; Alexander, A. J. Non-photochemical laser-induced nucleation of supercooled glacial acetic acid. *Phys. Chem. Chem. Phys.* **2012**, *14*, 90−93.
(27) Alexander, A. J.; Camp, P. J. Non-photochemical laser-induced nucleation. *J. Chem. Phys.* **2019**, *150*, 040901.
(28) Keller, R.; Beaver, L.; Prater, M. C.; Hord, N. G. Dietary Nitrate and Nitrite Concentrations in Food Patterns and Dietary Supplements. *Nut. Tod.* **2020**, *55*, 218−226.
(29) Laue, W.; Thiemann, M.; Scheibler, E.; Wiegand, K. W.*Nitrates and Nitrites;*Wiley-VCH: Weinheim, Germany, 2006.
(30) Burkinshaw, S. M.; Salihu, G. The role of auxiliaries in the immersion dyeing of textile fibers: Part 6 analysis of conventional models that describe the manner by which inorganic electrolytes promote reactive dye uptake on cellulosic fibers. *Dyes Pigm.* **2019**, *161*, 595−604.
(31) Stern, K. H.*High Temperature Properties and Thermal Decomposition of Inorganic Salts with Oxyanions;*CRC Press: Boca Raton, FL, 2001.
(32) Randolp, A.; Larson, M.*Theory of Particulate Processes;*Academic Press: New York, 1971.
(33) Mullin, J. W.*Crystallization,*4th ed.; Butterworth-Heinemann: London, UK, 2001.
(34) Kondepudi, D. K.; Prigogine, I.*Modern Thermodynamics,*2nd ed.; John Wiley, 2015.
(35) Sankin, G. N.; Zhou, Y.; Zhong, P. Focusing of Shockwaves Induced by Optical Breakdown in Water. *J. Acoust. Soc. Am.* **2008**, *123*, 4071−4081.
(36) Jacob, J. A.; Sorgues, S.; Dazzi, A.; Mostafavi, M.; Belloni, J. Homogeneous Nucleation-Growth Dynamics Induced by Single Laser Pulse in Supersaturated Solutions. *Cryst. Growth Des.* **2012**, *12*, 5980−5985.
(37) Hua, T.; Gowayed, O.; Grey-Stewart, D.; Garetz, B. A.; Hartman, R. L. Microfluidic Laser-Induced Nucleation of Supersaturated Aqueous KCl Solutions. *Cryst. Growth Des.* **2019**, *19*, 3491−3497.
(38) Ravindran, T. R.; Rajan, R.; Venkatesan, V. Review of Phase Transformations in Energetic Materials as a Function of Pressure and Temperature. *J. Phys. Chem. C* **2019**, *123*, 29067−29085.
(39) Dreger, Z. A.; Gruzdkov, Y. A.; Gupta, Y. M.; Dick, J. J. Shock Wave Induced Decomposition Chemistry of Pentaerythritol Tetranitrate Single Crystals: Time-Resolved Emission Spectroscopy. *J. Phys. Chem. B* **2002**, *106*, 247−256.

https://doi.org/10.1021/acsomega.2c03456
ACS Omega 2022, 7, 38400−38408